

Metal Selectivity of the *Escherichia coli* Nickel Metallochaperone, SlyD

Harini Kaluarachchi,[†] Judith F. Siebel,^{†,||} Supipi Kaluarachchi-Duffy,[‡] Sandra Krecisz,[†] Duncan E. K. Sutherland,[§] Martin J. Stillman,[§] and Deborah B. Zamble^{*,†}

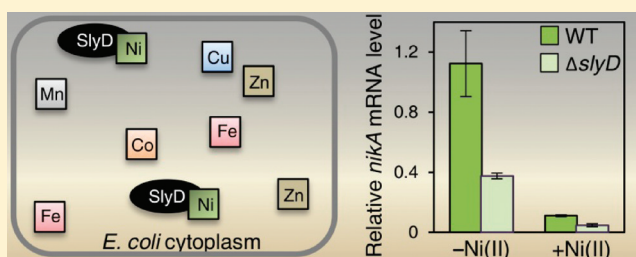
[†]Department of Chemistry, University of Toronto, Toronto, Ontario, Canada M5S 3H6

[‡]Department of Molecular Genetics, University of Toronto, Toronto, Ontario, Canada M5S 3E1

[§]Department of Chemistry, University of Western Ontario, London, Ontario, Canada N6A 5B7

S Supporting Information

ABSTRACT: SlyD is a Ni(II)-binding protein that contributes to nickel homeostasis in *Escherichia coli*. The C-terminal domain of SlyD contains a rich variety of metal-binding amino acids, suggesting broader metal binding capabilities, and previous work demonstrated that the protein can coordinate several types of first-row transition metals. However, the binding of SlyD to metals other than Ni(II) has not been previously characterized. To improve our understanding of the in vitro metal-binding activity of SlyD and how it correlates with the in vivo function of this protein, the interactions between SlyD and the series of biologically relevant transition metals [Mn(II), Fe(II), Co(II), Cu(I), and Zn(II)] were examined by using a combination of optical spectroscopy and mass spectrometry. Binding of SlyD to Mn(II) or Fe(II) ions was not detected, but the protein coordinates multiple ions of Co(II), Zn(II), and Cu(I) with appreciable affinity (K_D values in or below the nanomolar range), highlighting the promiscuous nature of this protein. The order of affinities of SlyD for the metals examined is as follows: Mn(II) and Fe(II) < Co(II) < Ni(II) ~ Zn(II) \ll Cu(I). Although the purified protein is unable to overcome the large thermodynamic preference for Cu(I) and exclude Zn(II) chelation in the presence of Ni(II), in vivo studies reveal a Ni(II)-specific function for the protein. Furthermore, these latter experiments support a specific role for SlyD as a [NiFe]-hydrogenase enzyme maturation factor. The implications of the divergence between the metal selectivity of SlyD in vitro and the specific activity in vivo are discussed.



Metal homeostasis is an essential yet complex process that is achieved through the action of a number of proteins often working in concert.^{1,2} These factors ensure that metal-dependent proteins are paired with the correct metal ion(s) to produce biologically active complexes. The proteins involved in metal homeostasis include membrane importers and exporters, metal storage proteins that are responsible for safe sequestration, metallochaperones dedicated to targeted delivery of metal ions, and metal-sensing transcription factors, which together control the amount of a specific metal available in the cellular cytoplasm. The fidelity of these proteins is at the top of a hierarchy of metal-selective processes, and their selectivity is proposed to ultimately influence the metal occupancy of all other proteins that require a metal ion cofactor for function.^{2,3} Therefore, a detailed understanding of the proteins involved in metal homeostasis and their ability to recognize and chelate a cognate metal partner is a prerequisite for deciphering how metal selectivity is achieved in the context of an entire cell.

Escherichia coli SlyD is an example of a protein that is involved in Ni(II) homeostasis. SlyD contributes to both nickel accumulation and energy metabolism in this organism because it participates in the Ni(II) insertion step during [NiFe]-hydrogenase metallocenter assembly.^{4,5} Nuclear magnetic

resonance (NMR) solution structures of *E. coli* SlyD revealed that the N-terminal region consists of two well-defined domains.^{6,7} The FKBP (FK-506 binding protein) domain has a structure similar to those of other members of the FKBP family of peptidyl-prolyl isomerases (PPIases) and catalyzes the isomerization of proline peptide bonds during protein folding.^{8,9} The IF (insert in the flap) domain recognizes and binds to unfolded protein, contributing to the protein folding activity.^{10,11} In addition, the final 50 residues at the C-terminus of SlyD correspond to the metal-binding domain (MBD) and include 28 potential metal-binding amino acids (6 Cys, 15 His, 2 Glu, and 5 Asp residues) (Figure S1 of the Supporting Information). This C-terminal domain remains unstructured according to NMR data and is variable between SlyD homologues.^{7,12} A vital role for the MBD of SlyD was established upon truncation of the protein in *E. coli*, which resulted in compromised hydrogenase production.¹³ In support of the nickel-related in vivo function of SlyD, a recent analysis

Received: September 23, 2011

Revised: November 1, 2011

Published: November 2, 2011



of the isolated protein demonstrated that it can bind up to seven Ni(II) ions with an affinity in the nanomolar range.¹⁴ This in vitro investigation also revealed that SlyD coordinates Ni(II) through a noncooperative mechanism and exists in a mixture of metalloforms at any given metal concentration. The ability of the unique MBD of SlyD to sequester a substantial amount of Ni(II) has been proposed to contribute to Ni(II) storage in *E. coli* and provide a source of Ni(II) for the hydrogenase enzymes.¹⁵

Previous in vitro analysis revealed that in addition to Ni(II), SlyD can bind at least substoichiometric amounts of other types of transition metals such as Zn(II), Cu(II), and Co(II).¹⁵ This finding is not surprising given the dense mix of different types of metal-binding amino acids in the MBD, which could feasibly meet the chemical coordination preferences of a range of metal ions. Thus, SlyD may contribute broadly to the homeostasis of other metal ions in *E. coli*. To test this hypothesis, we explored the metal-binding activity of SlyD to several biologically relevant first-row transition metals, Mn(II), Fe(II), Co(II), Cu(I), and Zn(II).¹⁶ Our results indicate that while SlyD does not bind Mn(II) or Fe(II) with appreciable affinity, it tightly binds to Co(II), Cu(I), and Zn(II) in addition to Ni(II). We also find that Ni(II) can replace Co(II) bound to SlyD but that selectivity for Ni(II) is not observed in the presence of Cu(I) or Zn(II). In contrast, although SlyD did not exhibit selectivity toward Ni(II) in vitro, in vivo experiments reveal that SlyD can specifically influence the balance of nickel ions in *E. coli* under anaerobic conditions, while it had no effect on factors required for the homeostasis of other types of metals. This discrepancy is discussed in the context of the *E. coli* cell and provides strong support for the assignment of SlyD as a dedicated nickel factor.

■ EXPERIMENTAL PROCEDURES

Materials. The following metal salts, ZnSO₄, [Cu(CH₃CN)₄]PF₆, Ni(acetate)₂, CoSO₄, FeSO₄, and MnCl₂, were purchased from Sigma-Aldrich at a minimum of 99.9% pure. Except for copper solutions, all metal solutions were prepared by dissolving the salts as purchased in Milli-Q water that was stirred in an anaerobic glovebox (<1 ppm O₂) for at least 24 h to minimize oxygen content. Concentrations of metal stock solutions were verified by ICP-AES. The Cu(I) salts were recrystallized as described previously to remove any trace amounts of Cu(II), and the resulting powder was dissolved in an Ar(g)-saturated 30% (v/v) acetonitrile/water solution.¹⁷ The concentrations of the copper solutions were established by using bathocuproine sulfonate (Bcs) as described previously.¹⁸ Buffers for all metal assays were prepared with Milli-Q water that was then treated with Chelex-100 (Bio-Rad) and stirred in an anaerobic glovebox (<1 ppm O₂) for at least 24 h prior to use. All titrations and assays were conducted in at least triplicate to ensure reproducibility. The metal chelators ethylene glycol tetraacetic acid (EGTA), bicinechoninate (Bca), Bcs, glycine and 4-(2-pyridylazo)resorcinol (PAR) were purchased from Sigma-Aldrich at a minimum of 99% pure, and the pH values of the stock solutions were adjusted to match that of the protein buffer.

Protein Expression, Purification, and Preparation. SlyD wild-type (WT) and triple-mutant proteins were expressed and purified as mentioned previously.¹⁴ The triple mutant was prepared to investigate the role of the six cysteine residues, which are present in the SlyD MBD in pairs. All three sets of cysteines have been removed from this mutant, which has the following mutations and deletions: Cys to Ala mutation

at positions 167, 168, 184, and 185 and removal of the last four residues (Δ 193–196). Preparation of the apoprotein and determination of the reduction state of the WT SlyD via *N*-ethylmaleimide modifications were conducted as described previously.¹⁴

Metal Binding via Electronic Absorption Spectroscopy. Protein samples were buffer exchanged into 20 mM HEPES (pH 7.5) and 100 mM NaCl, and 90 μ L aliquots of apo SlyD were incubated with the appropriate metal concentrations as noted at 4 °C under anaerobic conditions. Samples were analyzed under aerobic conditions except for Fe(II) and Cu(I) titrations, which were measured in an anaerobic cuvette to minimize exposure to air. Because of significant background signals from Fe(II) and Cu(I) in HEPES buffer, metal binding experiments for these two metals were conducted in 10 mM ammonium acetate (pH 7.5) that was bubbled with N₂(g). Experiments involving Cu(I) and Bcs or Bca were conducted in 20 mM HEPES buffer (pH 7.5) and 100 mM NaCl, and spectroscopic analysis was conducted under aerobic conditions.

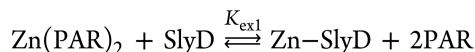
Equilibrium Dialysis. SlyD samples (40 μ M) were dialyzed against an equal volume of 320 μ M metal solutions at 4 °C overnight in an anaerobic glovebox using Microchambers of DIALYZER (Harvard Apparatus). At the end of the equilibration period, samples from the protein chamber (metal bound to protein and free metal) and the metal ion chamber (free metal) were measured in triplicate via a previously described high-performance liquid chromatography method.¹⁹

Metal Binding via ESI-MS. Protein samples were buffer exchanged using 500 μ L aliquots of 10 mM ammonium acetate (pH 7.5) in six dilution steps using 10K nanosep centrifugal devices (PALL Science). This volatile buffer is essential for acquiring clean MS data. Control experiments were conducted to ensure that results obtained when using ammonium acetate as a buffer were comparable to those obtained using 20 mM HEPES (pH 7.4) and 100 mM NaCl. Direct metal titration results for Zn(II) were obtained by equilibrating the protein samples (10 μ M each) with a known amount of ZnSO₄. Titrations of SlyD with Cu(I) and Co(II) were realized by incubating the protein samples (10 μ M) with [Cu(MeCN)₄]⁺ or CoSO₄ in the presence of 100 μ M DTT. Samples were allowed to equilibrate overnight at 4 °C in an anaerobic glovebox, followed by transfer to septum-capped vials for MS analysis.

ESI-MS Instrumental Parameters and Data Acquisition and Processing. The mass spectra were recorded on an AB/Sciex QStarXL mass spectrometer equipped with an ion spray source in the positive ion mode and a hot source-induced desolvation (HSID) interface (Ionics Mass Spectrometry Group Inc.). The HSID is an atmospheric-pressure interface that is used for efficient desolvation of a sample that is accomplished via the transfer of energy from the hot gas as the ions travel through multiple flow regions. The resulting ions are orthogonally introduced into the mass spectrometer, and the interface is expected to lead to greater sensitivity and stability of the signal while operating like a conventional ion source. Ions were scanned from *m/z* 1300 to 3000 with accumulation of 1 s per spectrum with no interscan time delay and averaged for a 2–4 min period. The instrument parameters were set as follows: ion source temperature, 200 °C; ion source gas, 50.0 psi; curtain gas, 50.0 psi; ion spray voltage, 5000.0 V; declustering potential, 60.0 V; focusing potential, 60 V; collision gas, 3.0; MCP (detector), 2200.0 V. The spectra

were deconvoluted using the Bayesian protein reconstruction program over a mass range of 20000–22000 Da and a mass step of 1 Da, and a signal:noise ratio of 20 and a detected minimal intensity of 1% were used during reconstruction of the data. The addition of DTT to protein samples decreases the intensity of the signals detected, and at metal concentrations of ≥ 2 equiv of metal (i.e., $\geq 20 \mu\text{M}$), the signal is further suppressed because of the high-salt conditions. Therefore, samples containing DTT were acquired with instrument conditions similar to those listed above except the Q1 transmission was enhanced at m/z 2500. The amounts of apo and holo SlyD species were calculated from the signal intensities of the reconstructed spectra assuming that all of the metalloforms are ionized to the same extent. Only the peaks corresponding to salt-free SlyD were used for calculating the metalation states of SlyD.

Competition Experiments for Determining the K_D . To determine the affinity of SlyD for Zn(II), a competition reaction was set up as noted in the following equation by adding increasing amounts of apo SlyD to separate aliquots of 400 μM PAR containing 8 μM Zn(II) in 20 mM HEPES (pH 7.5) and 100 mM NaCl.



Samples were equilibrated overnight at 4 °C and subsequently analyzed by electronic absorption spectroscopy at 500 nm. Titrations of 400 μM PAR with Zn(II) under identical conditions were used to calculate the amount of $\text{Zn}(\text{PAR})_2$ formed in the competition described above. As the pH of the solution greatly affects the formation constant as well as the molar absorption coefficient (ϵ) of the $\text{Zn}(\text{PAR})_2$ complex, the metal binding affinity of PAR under these particular buffer conditions was calibrated by using EGTA as described in detail by Zimmerman et al.¹⁸ Further details of the competition reactions are given in the Supporting Information.

To determine the affinity of SlyD for Cu(I), apo SlyD was titrated into a solution of $[\text{Cu}(\text{Bcs})_2]^{3-}$ with a defined Bcs:Cu(I) molar ratio of ≥ 2.5 . Transfer of Cu(I) from the chelator to protein or vice versa can be detected by the change in absorbance at 483 nm for Bcs.¹⁸ By systematically varying the concentration of the chelators and the protein, we achieved conditions that favored competition, and the resulting spectra were used for calculating the K_D . For additional information, see the Supporting Information.

To determine the affinity of SlyD for Co(II), separate aliquots of 35 μM Fura2 (Invitrogen) containing 8–12 μM Co(II) were titrated with apo SlyD. The resulting solutions were analyzed using electronic absorption spectroscopy at 368 nm, and this titration was compared to titration of Fura2 with CoSO_4 under identical conditions to establish the concentration of Co-Fura2 in each sample. An average K_D was calculated using data from several replicates. For additional details, see the Supporting Information.

Circular Dichroism (CD) Spectroscopy. Apo SlyD (60 μM) was buffer exchanged into 10 mM ammonium acetate (pH 7.5) using 10K nanosep centrifugal devices (PALL Science) and incubated with known amounts of metal overnight at 4 °C in an anaerobic glovebox. Samples were loaded into a 0.1 cm cuvette and capped to minimize exposure to air. The spectra were recorded on a Jasco J-710 spectropolarimeter by scanning from 205 to 320 nm at room temperature. The final spectra

obtained are averages of five scans collected by using a scan speed of 20 nm/min.

Cu(I) Binding Stoichiometry Using Bca. Apoprotein samples were titrated into a solution of $[\text{Cu}(\text{Bca})_2]^{3-}$ with a defined L:Cu(I) molar ratio of ≥ 2.5 , in which the ligand and copper concentrations were held constant. Transfer of Cu(I) from the chelator to protein or vice versa can be detected by monitoring the change in absorbance at 562 nm for Bca.¹⁸ By systematically varying the concentration of Bca and the protein, we achieved conditions that disfavored competition.

Metal Toxicity Studies. In *LB Media*. Wild-type and ΔslyD strains from the BW25113 KEIO gene deletion collection were used in this assay.²⁰ The growth rates of wild-type and ΔslyD strains under different metal concentrations were assessed by measuring the OD_{600} over 24 h. The following metal salts were utilized to supplement the growth media: NiCl_2 , CoSO_4 , ZnSO_4 , and CuSO_4 . All cultures were maintained at 37 °C in an aerobic environment. The concentrations tested are summarized in Table S1 of the Supporting Information.

In *Minimal Media*. All solutions used in this assay were treated with Chelex-100 overnight to remove any trace metals. Metal stocks were prepared from Chelex-treated Milli-Q water. The M9 medium (1 \times) (Sigma) was supplemented with 0.2% glucose, 1 mM MgSO_4 , and 100 μM CaCl_2 and sterile filtered (minimal medium). Two wild-type bacterial strains were used in these toxicity studies, the above-mentioned BW25113 and MC4100, as well as the corresponding ΔslyD strains. The growth rates were monitored in M9 medium by measuring the OD_{600} over 24 h. All cultures were maintained at 37 °C under aerobic conditions. The concentrations of metals tested are summarized in Table S1 of the Supporting Information.

Growth Conditions for Quantitative Real-Time Polymerase Chain Reaction (qRT-PCR). *Aerobic.* All experiments were conducted using the MC4100 bacterial strain and the ΔslyD strain in the same background.⁵ Cultures were grown in minimal medium at 37 °C with aerobic shaking at 250 rpm until the cultures reached the exponential growth phase (approximately 16 h) followed by treatment with a known amount of metal for 30 min.

Anaerobic. For anaerobic growth experiments, MC4100 wild-type and ΔslyD strains were used. The M9 salts (1 \times) were treated with Chelex overnight to remove any trace metal, and then the following nutrients were added back to the medium: 30 mM sodium formate, 0.5% (v/v) glucose, 1 mM MgCl_2 , 100 nM CaCl_2 , 100 nM $(\text{NH}_4)_2\text{MoO}_4$, and 100 nM NaSeO_3 . Cultures were grown in a capped bottle without any headspace for 17 h at 37 °C, allowing the cultures to reach a midlog phase. These anaerobically grown cultures were then divided into sterile Falcon tubes containing no metal or with 10 μM NiCl_2 in an anaerobic glovebox. The small cultures were then capped and allowed to grow for an additional 30 min at 37 °C. For analysis of Zn(II) and Cu(II) under anaerobic conditions, an identical procedure was followed, except the Chelex-treated M9 medium was supplemented with only 0.2% (v/v) glucose, 1 mM MgCl_2 , and 100 nM CaCl_2 .

RNA Isolation and qRT-PCR. Total RNA was isolated by using the RNeasy Mini Kit (Qiagen) according to the manufacturer's protocol for the mechanical disruption and purification of bacterial RNA. The QuantiTect Reverse Transcription Kit (Qiagen) was used for synthesis of cDNA from ~ 0.5 –1 μg of RNA and to eliminate contaminating genomic DNA. qPCRs were performed on a LightCycler 480

Real-time PCR block (Roche) using SYBR green (Finnzymes) and primers specific for each transporter as listed in Table S2 of the Supporting Information. *holB* mRNA, encoding a DNA gyrase, was used as an internal control because the expression level of this protein is unaffected by metal supplementation.²¹

RESULTS

Zn(II) Binding to SlyD. Zn(II) is one of the transition metals most avidly acquired by *E. coli*, and the intracellular concentrations of this metal ion can reach up to ~0.1 mM.²² Furthermore, given the ligand composition of the SlyD MBD (Figure S1 of the Supporting Information), which contains a distribution of cysteine and histidine residues, it was feasible that the softer Zn(II) ion would bind readily to SlyD. We first examined binding of Zn(II) to SlyD in vitro by using mass spectrometry to analyze a titration experiment (Figure 1). The

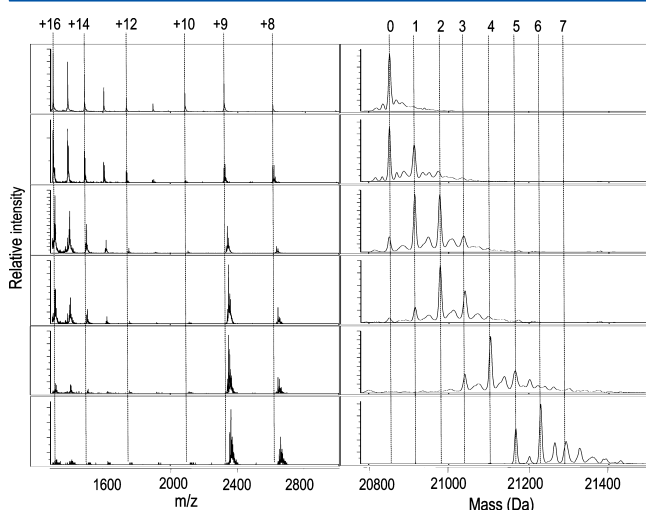


Figure 1. ESI-MS of titration of SlyD with Zn(II). The addition of increasing amounts of Zn(II) to SlyD (10 μ M) leads to concurrent filling of multiple metal sites indicating a noncooperative metal binding mechanism. From top to bottom, the numbers of equivalents of Zn(II) added relative to protein concentration are 0, 0.5, 1.5, 2, 4, and 6.3, respectively. The m/z spectra are shown on the left with the respective reconstructed spectra on the right. The numbers heading the dotted lines indicate the number of Zn(II) ions bound to SlyD (right) and the charge states of the protein (left).

data reveal several metalloforms of the protein that differ in the number of Zn(II) ions bound at each titration point, indicating that SlyD contains multiple metal-binding sites. The existence of these stable, partially metalated intermediates reflects a noncooperative metalation mechanism similar to that of binding of Ni(II) to SlyD.^{14,23}

Recently, a change in charge state distribution has been recognized as a sensitive indicator of protein structure.²⁴ Higher-numbered charge states, with smaller m/z values, represent a greater surface area than the lower-numbered series, and this can be interpreted as a more open structure. Changes in charge states observed during ESI-MS analysis as a function of metalation may indicate the formation of a structure that is folding around the metal-binding site.²⁴ The m/z spectrum of apo SlyD reveals two different populations of SlyD in solution (Figure 1 and Figure S2 of the Supporting Information), with most of the protein carrying a higher charge (i.e., the +16 charge state is more intense than the signal for the +9 species) indicating that apo SlyD predominantly

exists in a more unfolded population under these experimental conditions. Upon titration with Zn(II), the relative peak intensities for the species with the higher charge states decrease, suggesting a metal-induced conformational change that shifts the equilibrium to the more folded conformer.

The charge distribution observed for the apoprotein is slightly different than that from our previous study, in which a higher abundance of lower charge states was observed.¹⁴ The experiments reported here were conducted on the same instrument under identical experimental conditions but following installation of an HSID interface. This interface results in desolvation at higher temperatures, which could affect the populations of protein conformations detected. Therefore, to allow for a comparison of data acquired under the same instrumental settings, coordination of Ni(II) to SlyD was re-evaluated on the mass spectrometer equipped with the interface. As reported previously, the addition of Ni(II) caused a shift in the charge state envelopes to predominantly +8 and +9, indicating metal-induced folding similar to that caused by Zn(II) (Figure S2 of the Supporting Information and ref 14). These new data support our previous findings and unambiguously show the noncooperative binding of up to seven Ni(II) ions, as described above for Zn(II).

A definitive end point to the Zn(II) titration cannot be achieved by MS because the concentration of salt interferes with the quality of the data. Therefore, the total number of tight binding sites on SlyD was established by analyzing a protein sample that was treated with an 8-fold excess of Zn(II) overnight followed by gel-filtration chromatography to remove excess or loosely bound Zn(II). The mass spectrum indicates the presence of a mixed population of metalated species with a maximum of five metal-binding sites and dominant peaks arising from the four and five Zn(II)-coordinated species

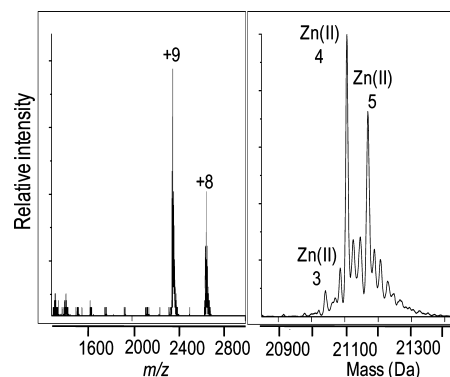


Figure 2. Zn(II) stoichiometry of SlyD. The mass spectrum of a solution of SlyD (100 μ M) incubated with 800 μ M Zn(II) followed by gel filtration to remove any weak or nonspecifically bound metal indicates a maximum capacity of five Zn(II) ions.

(Figure 2). These results indicate that the affinity of additional zinc ions is sufficiently low that they are lost on the column.

To estimate the affinity of SlyD for Zn(II), a competition assay was performed using the colorimetric indicator PAR. This chelator forms a 2:1 PAR–Zn(II) complex in solution that results in an increased absorbance at 500 nm.²⁵ Titration of apo SlyD into a 400 μ M PAR solution containing 8 μ M Zn(II) results in a nonlinear decrease in the magnitude of the signal at 500 nm, indicative of an effective competition between the protein and the ligand for Zn(II) (Figure S3 of the Supporting

Information). An identical titration with EGTA instead of protein was also conducted to calibrate the affinity of the $\text{Zn}(\text{PAR})_2$ complex under the buffer conditions used, because the formation constant of this complex is affected by the pH.¹⁸ The resulting data from these two titrations were fitted to a model assuming a single binding event, yielding an apparent K_D of $(1.0 \pm 0.4) \times 10^{-10}$ M (Table 1 and Figure S3 of the Supporting Information).

Table 1. Affinities of Metals for SlyD^a

metal	K_{Me} (M)
Co(II)	$(4 \pm 1) \times 10^{-9b}$
Ni(II)	$\leq 10^{-10c}$
Cu(I)	$(1.5 \pm 0.3) \times 10^{-17d}$
Zn(II)	$(1.0 \pm 0.1) \times 10^{-10e}$

^aThe data were treated by assuming binding of a single metal ion to obtain a macroscopic K_D . ^bDetermined via competition with Fura2. ^cEstimated from competition with PAR, Fura2, and the Zn –SlyD complex. ^dDetermined by competition with Bcs. ^eCalculated from competition experiments with PAR.

For comparison, the affinity of the $\text{Ni}(\text{II})$ –SlyD complex was also examined in more detail. Exploratory experiments indicated that the protein could compete with Fura2 ($K_D = 2.4 \times 10^{-8}$ M²⁶) for $\text{Ni}(\text{II})$ coordination (data not shown), establishing a quantitative upper limit to $\text{Ni}(\text{II})$ –SlyD complexes. Combining this result with the fact that $\text{Ni}(\text{II})$ can bind to SlyD concurrently with $\text{Zn}(\text{II})$ (see below) and compete with EGTA at low chelator concentrations,¹⁴ a $K_{D[\text{Ni}(\text{II})\text{--SlyD}]}$ of $\leq 10^{-10}$ M was estimated (Table 1).

To determine whether the $\text{Zn}(\text{II})$ –induced structural changes of SlyD suggested by ESI-MS match those induced by $\text{Ni}(\text{II})$ binding, we analyzed a $\text{Zn}(\text{II})$ titration by using CD spectroscopy. Two minima are observed for the apoprotein at 215 and 227 nm (Figure S4 of the Supporting Information). Typical β -sheet structures give rise to the band at 215 nm, as would be expected for SlyD because both the PPIase and IF domains are predominantly composed of β -sheets,⁷ whereas the 227 nm band suggests the presence of β -turn-type structures.^{27,28} As SlyD is titrated with $\text{Zn}(\text{II})$, a gradual decrease in the molar ellipticity is observed in the far-UV region that reaches a plateau upon addition of 4 molar equiv of $\text{Zn}(\text{II})$. Although this trend is similar to that observed when SlyD chelates $\text{Ni}(\text{II})$, the overall degree of change in the molar ellipticity is significantly lower for $\text{Zn}(\text{II})$. Therefore, the CD spectra suggest that the $\text{Zn}(\text{II})$ –induced secondary structure for SlyD is likely different from that of $\text{Ni}(\text{II})$.

To assess the selectivity of SlyD for $\text{Zn}(\text{II})$ or $\text{Ni}(\text{II})$, a competition titration was conducted in which apo SlyD was incubated with $\text{Ni}(\text{II})$ and $\text{Zn}(\text{II})$ overnight. Binding of $\text{Zn}(\text{II})$ to the protein could be monitored indirectly because replacement of $\text{Ni}(\text{II})$ with $\text{Zn}(\text{II})$ results in a decrease in the ligand to metal charge transfer (LMCT) band of the $\text{Ni}(\text{II})$ –SlyD complex at 315 nm.¹⁴ A less intense signal is observed when apo SlyD is titrated with an equimolar solution of $\text{Ni}(\text{II})$ and $\text{Zn}(\text{II})$ in comparison to titration with $\text{Ni}(\text{II})$ alone (Figure 3A). Thus, the data provide evidence for metal-binding sites on SlyD that preferentially sequester $\text{Zn}(\text{II})$ in the presence of $\text{Ni}(\text{II})$. To assess whether the order of metal addition affects the metalation state of SlyD, we conducted two competition titrations. SlyD was preincubated with an 8-fold excess of $\text{Ni}(\text{II})$ or $\text{Zn}(\text{II})$ for 24 h followed by titration with the other

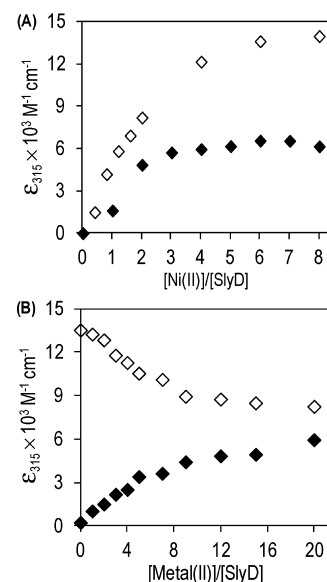


Figure 3. Selectivity of SlyD for $\text{Ni}(\text{II})$ vs $\text{Zn}(\text{II})$. (A) Addition of an equimolar solution of $\text{Ni}(\text{II})$ and $\text{Zn}(\text{II})$ to SlyD (◆) results in lower intensity at 315 nm when compared to that for a titration with equivalent amounts of $\text{Ni}(\text{II})$ alone (◇). The x-axis indicates the total amount of $\text{Ni}(\text{II})$ added relative to apo SlyD (15 μM). (B) Change in absorbance at 315 nm as $\text{Ni}(\text{II})$ is added to a SlyD sample (15 μM) preincubated with 8 molar equiv of $\text{Zn}(\text{II})$ (◆) or as $\text{Zn}(\text{II})$ is added to a SlyD sample preincubated with 8 molar equiv of $\text{Ni}(\text{II})$ (◇).

metal, and $\text{Ni}(\text{II})$ binding was monitored at 315 nm. A representative data set for each of the competition titrations that were allowed to equilibrate for 24 h after the addition of the second metal ion is shown in Figure 3B. Increasing the incubation period after addition of the second metal to 48 or 72 h generated similar results, suggesting that 24 h is sufficient to reach a thermodynamic equilibrium (data not shown). The results clearly demonstrate that $\text{Ni}(\text{II})$ is able to replace a fraction of the $\text{Zn}(\text{II})$ bound to SlyD and vice versa. Furthermore, the two titration curves do not intersect at any of the metal concentrations tested, highlighting that the metalation state of SlyD is dependent on the order of metal addition when considering $\text{Ni}(\text{II})$ and $\text{Zn}(\text{II})$. This result is consistent with a model in which the binding of the first metal ion locks the protein in a specific conformation, such that only a few of the remaining sites are then accessible for metal exchange reactions, as suggested by previous studies with nickel.¹⁴

Cu(I) Binding to SlyD. Compared to that of zinc, the intracellular quota of copper is lower in *E. coli* but still appreciable, reaching ~ 10 μM .²² As SlyD is a cytoplasmic protein, we characterized only binding of Cu(I) to the protein in detail [not Cu(II)] because this is likely the prevalent form of copper present in the reducing cytosolic environment.²⁹ Addition of Cu(I) to SlyD is accompanied by a charge transfer band in the electronic absorption spectrum centered around 254 nm that reaches saturation at 5 equiv of metal added (Figure S5 of the Supporting Information). There is precedence for binding of electron rich Cu(I) to the softer thiolate ligands, and the 254 nm signal is ascribed to a $\text{S} \rightarrow \text{Cu}(\text{I})$ charge transfer band.^{30,31} To verify this assignment, we conducted a similar titration of a SlyD mutant devoid of all Cys residues (termed the triple mutant because all three pairs of cysteines of SlyD have been removed¹⁴). The addition of Cu(I)

to the mutant SlyD failed to generate a change in the absorption spectrum (data not shown), suggesting that the LMCT bands are due to binding of Cu(I) to SlyD via thiolate residues.

To gain an understanding of the Cu(I) binding mechanism of SlyD, we analyzed copper titrations via ESI-MS. Although all possible precautions were taken to ensure anaerobic conditions, the addition of Cu(I) resulted in the appearance of protein dimers that were accompanied by a decrease in the protein mass by 6 Da (data not shown), suggesting oxidation of the protein. Titration of SlyD with Cu(II) followed by MS analysis revealed similar results, so further analysis with Cu(II) was not performed. Instead, copper titrations of SlyD were re-evaluated in the presence of 100 μ M DTT. Inclusion of the reducing agent did indeed prevent the formation of protein dimers and the accompanying loss of mass (Figure 4 and data not shown),

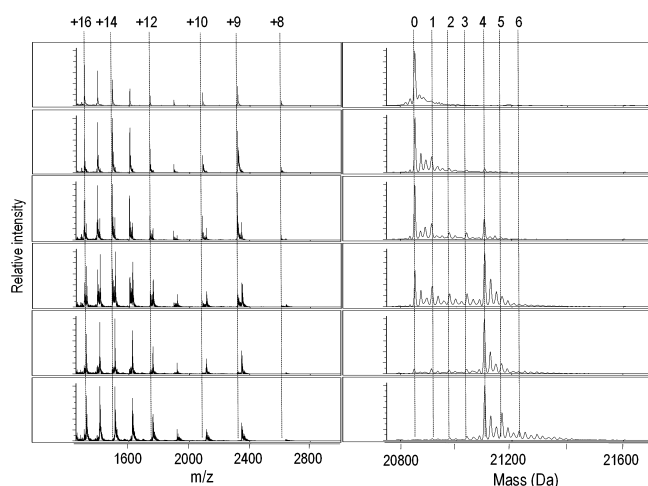


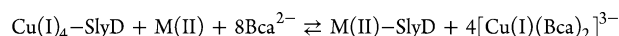
Figure 4. ESI-MS of titration of SlyD with Cu(I) in the presence of 100 μ M DTT. The addition of increasing amounts of Cu(I) to SlyD (10 μ M) leads to the appearance of several Cu(I)–SlyD species. From top to bottom, the numbers of equivalents of Cu(I) added relative to protein concentrations are 0, 0.3, 0.8, 2.3, 3.9, and 6, respectively. The m/z spectra are shown on the left with the respective reconstructed spectra on the right. The numbers heading the dotted lines indicate the number of Cu(I) ions bound to SlyD (right) and the charge states of the protein (left). The most intense peaks correspond to apo, one-Cu(I)-bound, and four-Cu(I)-bound SlyD species [with <4 equiv of Cu(I)].

but it significantly reduced the magnitude of the ion signal detected, resulting in spectra with poor resolution (data not shown). Therefore, to improve the quality of the spectra, we conducted Cu(I) titrations containing DTT in the buffer with the ion signal enhanced at m/z 2500 (Figure 4). Upon titration with <4 molar equiv of Cu(I), the predominant species observed correspond to apo SlyD, a small amount of SlyD with a single copper ion bound, and SlyD with four Cu(I) ions bound. Assuming that all metal–SlyD species are ionized to the same extent, this metalation pattern implies that binding of a single Cu(I) ion to the protein facilitates the binding of the second, third, and fourth Cu(I) ions through a partially cooperative mechanism, unlike Ni(II) and Zn(II). However, it is not possible to rule out the possibility that this pattern of metalation is due to the decreased stability of the lower metalated Cu(I) species [i.e., fewer than four Cu(I) ions] in the MS. The addition of 6 molar equiv of Cu(I) results in the appearance of metalloforms with more than four Cu(I) ions

bound, but a definitive saturation point could not be obtained through this direct titration method as the higher concentrations of salt interfere with the quality of the MS data. It should be noted that significant changes in the population of charge states are not detected when Cu(I) is added. This observation is due to the above-mentioned enhancement of the signal at m/z 2500, because Ni(II) titrations analyzed under these instrument settings did not reveal the expected shift in the m/z spectra (Figure S2 of the Supporting Information and data not shown).

Given that ESI-MS could not be used to determine the Cu(I) stoichiometry, coupled with the fact that binding of Cu(I) to SlyD was analyzed in the presence of DTT, which has a considerable affinity for Cu(I),³² the stoichiometry of the metal complex was re-evaluated by using the small molecule chelator Bca. This copper probe forms an air-stable $[\text{Cu}(\text{Bca})_2]^{3-}$ complex with a formation constant β_2 of $10^{17.2}$ and gives rise to a charge transfer band in the visible region with a maximum at 562 nm ($\epsilon = 7900 \text{ M}^{-1} \text{ cm}^{-1}$).¹⁸ Titration of wild-type apoprotein into a solution of 40 μ M Cu(I) and 100 μ M Bca [or 300 μ M (data not shown)] resulted in a linear decrease in the magnitude of the signal at 562 nm, indicating noncompetitive conditions (inset of Figure S6 of the Supporting Information). A linear fit of the data reveals that 10 μ M SlyD is sufficient to remove the 40 μ M Cu(I) bound to Bca, thereby confirming that the protein binds 4 equiv of Cu(I) (Figure S6 of the Supporting Information). To determine the $K_{\text{Cu(I)}}$ of SlyD, competitive conditions were achieved by using the Bcs chelator. Similar to Bca, Bcs also coordinates Cu(I) to form an air-stable $[\text{Cu}(\text{Bcs})_2]^{3-}$ complex, albeit with a higher formation constant ($\beta_2 = 10^{19.8}$), which can be detected by a charge transfer band with a maximum at 483 nm ($\epsilon = 13000 \text{ M}^{-1} \text{ cm}^{-1}$).¹⁸ Titrations of protein into a solution containing constant concentrations of Bcs and copper at 300 and 40 μ M, respectively (Figure S7 of the Supporting Information), were fitted assuming a single binding scheme to obtain an apparent K_D of $(1.5 \pm 0.3) \times 10^{-17} \text{ M}$ for binding of Cu(I) to SlyD.

To evaluate the metal selectivity of SlyD with respect to Cu(I), a second series of experiments were conducted using the weaker copper probe, Bca. To establish whether the reaction described below can occur, 10 μ M SlyD was first incubated with 50 μ M Cu(I) for 1 h, followed by addition of 200 μ M Bca. Then 80 μ M Ni(II) or Zn(II) was added and the mixture allowed to equilibrate for 24 h.



As expected, the addition of Bca to the SlyD sample leads to an increase in the absorption at 562 nm corresponding to a concentration of 10 μ M $[\text{Cu}^{\text{I}}(\text{Bca})_2]^{3-}$ (data not shown). However, neither excess Ni(II) nor Zn(II) affected the signal at 562 nm, demonstrating that the forward reaction described above did not occur under these experimental conditions (data not shown). Control experiments were conducted with Bca and Ni(II) or Zn(II) alone to ensure that neither of these metals alters the spectrum of Bca. To determine if the reverse reaction could be conducted, a 10 μ M protein sample was preincubated with 8 equiv of Ni(II) or Zn(II) for 24 h, followed by addition of 5 equiv of Cu(I) and 200 μ M Bca and equilibration for an additional 24 h. The resulting signal at 562 nm corresponded to only 10 μ M $[\text{Cu}^{\text{I}}(\text{Bca})_2]^{3-}$, suggesting that 40 μ M Cu(I) was bound by SlyD (data not shown). Therefore, these results support tight binding of four Cu(I) ions even in the presence of Ni(II) or Zn(II). This preferential binding of Cu(I)

corroborates the binding constants measured for the different metals thus far, where $K_{D[Cu(I)-SlyD]} < K_{D[Ni(II)-SlyD]}$ and $K_{D[Zn-SlyD]}$.

Co(II) Binding to SlyD. Although cobalt is not widely used by *E. coli*, this transition metal ion can still be found in low abundance in the cytosol of this bacteria.¹⁶ In addition, Co(II) was of particular interest to us because two other proteins involved in nickel homeostasis, RcnR and RcnA, also contribute to cobalt homeostasis in *E. coli*.^{33–35} To determine whether SlyD could coordinate Co(II), a direct cobalt titration of apo SlyD was analyzed via electronic absorption spectroscopy (Figure 5). The addition of Co(II) leads to an increase in the

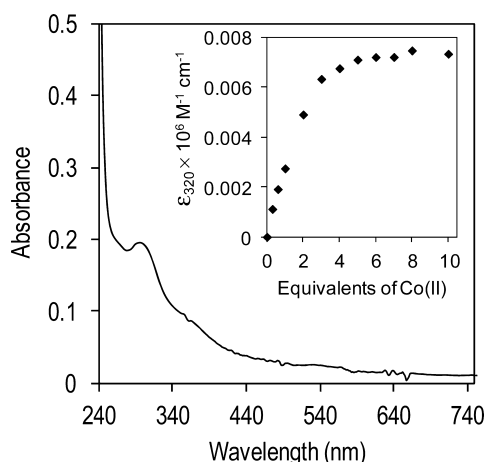


Figure 5. Co(II) binding to SlyD. Difference spectrum generated by subtracting apo SlyD (25 μ M) from a protein sample incubated with 7 equiv of Co(II). The inset is a plot of the molar absorptivity at 320 nm vs the number of equivalents of Co(II) and indicates saturation around 3–4 equiv of Co(II) added.

absorption at 280 nm accompanied by a broad shoulder in the 300–390 nm region that saturates upon addition of 3–4 equiv of the metal (Figure 5, inset). The spectrum of the Co(II)-saturated SlyD sample reveals an LMCT band at 293 nm ($\epsilon_c = 7800 \text{ M}^{-1} \text{ cm}^{-1}$) and a broader charge transfer band centered around 360 nm ($\epsilon_c = 3418 \text{ M}^{-1} \text{ cm}^{-1}$) [the linear increase in absorption upon addition of Co(II) was used to determine the molar absorptivity of the metal–protein complex]. These electronic absorption bands are attributed to LMCT from thiolates to the metal center,^{33,36} an assignment supported by the lack of such a CT band when Co(II) is added to the triple mutant (data not shown), and the intensity of these near UV bands suggests that all six Cys residues contribute to cobalt coordination.

To evaluate Co(II) binding in more depth, we used ESI-MS. Similar to the copper titrations described above, the addition of cobalt ions led to a concomitant decrease in the mass of the protein by 6 Da and the appearance of dimeric species (data not shown), indicating oxidation of the protein. Therefore, titrations were conducted in the presence of 100 μ M DTT. Mass spectrometry data revealed that like the Ni(II) and Zn(II) titrations, Co(II) binding by the protein occurred through a noncooperative mechanism that produced mixtures of metalated species at all Co(II) concentrations tested (Figure S8 of the Supporting Information). At a given amount of Co(II), lower stoichiometries of Co(II)–SlyD species were observed for samples containing DTT than for samples without DTT, indicating that the reducing agent was competing with SlyD for

cobalt ion binding (data not shown). Therefore, the stoichiometry of the protein for Co(II) was established through equilibrium dialysis, which indicated an average of four Co(II) ions bound per monomer, a capacity analogous to that of Ni(II) (Table S3 of the Supporting Information).

To determine the affinity of SlyD for Co(II), we performed competition experiments with the fluorescence indicator Fura2. Although Fura2 was originally designed as a molecular sensor for Ca(II), this chelator has also been used for determining the affinity of several proteins for various transition metals, including Co(II).^{36,37} The chelator forms a 1:1 complex with Co(II) that can be detected by the decrease in absorbance at 368 nm. Competitive conditions required for determining the dissociation constant of SlyD for cobalt ions were achieved by titrating apoprotein into a constant concentration of the Co(II)–Fura2 complex, leading to an increase in the magnitude of the signal at 368 nm (indicative of a decreasing Co(II)–Fura2 complex concentration in solution) (Figure S9 of the Supporting Information). To determine the affinity, data with a fractional saturation between 0.8 and 0.2 (with respect to the Fura2 complex) from several replicates were compiled to yield an average $K_{D[SlyD-Co(II)]}$ of $(4 \pm 1) \times 10^{-9} \text{ M}$ (Table 1). It should be noted that we used the K_D of $8.64 \times 10^{-9} \text{ M}$ reported for the Co(II)–Fura2 complex at pH 7.0,³⁸ because the affinity of this chelator for metal is constant near neutral pH.³⁹

To establish the metal selectivity of SlyD for Co(II) versus Ni(II), equilibrium dialysis was used. Metal analysis of samples equilibrated with 8-fold amounts of both Co(II) and Ni(II) revealed that the protein was exclusively bound to Ni(II) with an average stoichiometry of 4.4 (Table S3 of the Supporting Information). Given that SlyD binds an average of approximately four Ni(II) ions when equilibrated with Ni(II) alone (Table S3 of the Supporting Information and ref 14), these data indicate that SlyD selectively coordinates Ni(II) to its full capacity in the presence of Co(II). Similarly, titration of Zn(II) into a sample of SlyD preincubated with an 8-fold excess of Co(II) caused the LMCT band at 320 nm to disappear completely at 6 equiv of Zn(II) added, indicating effective replacement of Co(II) with Zn(II) at metal sites composed of Cys ligands (Figure S10 of the Supporting Information).

Fe(II) Binding to SlyD. The high iron quota of *E. coli*, ~0.1 mM,¹⁶ and the propensity of this metal to coordinate to Cys residues suggested that binding of Fe(II) to SlyD was also likely. However, electronic absorption spectroscopy of SlyD titrated with Fe(II) did not reveal any changes in the spectrum of apo SlyD (data not shown). Given that Fe(II) binding to thiolate ligands is expected to generate LMCT or MLCT bands in the visible or UV regions of the absorption spectrum,⁴⁰ this result suggests that SlyD does not bind Fe(II) under the experimental conditions used. In support of this conclusion, Ni(II) binding to SlyD was unaffected by preincubation with 10 molar equiv of Fe(II) (Figure S11 of the Supporting Information).

Mn(II) Binding to SlyD. Considering the large number of carboxylate and His residues present in SlyD, Mn(II) is another metal ion that could be coordinated by this protein. The addition of Mn(II) to SlyD did not produce any change in the electronic absorption profile of the protein (data not shown), and equilibrium dialysis revealed only a small fraction of the protein bound to the metal (Table S3 of the Supporting Information). Furthermore, the presence of Mn(II) did not affect binding of Ni(II) to SlyD monitored by electronic

absorption spectroscopy (data not shown) or metal analysis (Table S3 of the Supporting Information).

Susceptibility of Δ slyD *E. coli* to External Metal Concentrations. The metal binding data described above demonstrate that SlyD can coordinate several different types of metal ions in vitro with considerable affinity, so it was feasible that SlyD plays a role in minimizing the effects of metals in *E. coli* by functioning as a general metal buffer or detoxifier and a metal ion sink. To test this hypothesis, we examined the growth rates of wild-type and Δ slyD strains in either LB or minimal medium supplemented with different metals (Table S1 of the Supporting Information) by monitoring the optical density. The amounts of metals used were sufficient to inhibit growth of the bacteria, but no significant differences in the growth rates were observed for the Δ slyD strain compared to the wild-type strain at any of the metal concentrations tested (Figure S12 of the Supporting Information and data not shown), suggesting that SlyD does not confer metal resistance against cobalt, nickel, copper, or zinc in *E. coli* under aerobic growth conditions.

Impact of the slyD Deletion on Transcriptional Metalloregulators. To assess the role of SlyD in metal homeostasis, we examined the transcription of several metal transporters in *E. coli* by using qRT-PCR. The expression of these proteins is tightly regulated by metal-sensing transcription factors that gauge the available concentrations of a particular metal with extreme selectivity.⁴¹ Thus, a comparison between the mRNA levels of wild-type and Δ slyD strains should allow us to determine if there is an impact of SlyD on a given metal homeostasis pathway. SlyD appears to be constitutively expressed in *E. coli* in the presence or absence of oxygen,⁵ a variable that might modulate the metal requirements of the bacteria, so we examined the effects of SlyD under both conditions. Given that SlyD is connected to nickel biochemistry as an accessory protein for Ni(II) delivery during biosynthesis of the [NiFe]-hydrogenase enzymes,⁵ we hypothesized that SlyD could lead to perturbation of the nickel ion balance in *E. coli*. Furthermore, because SlyD can bind multiple Zn(II) or Cu(I) ions with affinities equal to or greater than that for Ni(II), we also examined the contribution of SlyD in the homeostasis of these metals.

While a specific Ni(II) uptake system is not known to be expressed under aerobic conditions, Ni(II) can still gain access to the cytoplasm in the presence of oxygen through nonspecific metal importers such as CorA or other unidentified means.¹ Repression of the gene encoding the Ni(II) exporter RcnA by the metalloregulator RcnR is alleviated in response to nickel, an effect observed in the presence or absence of oxygen.⁴² As expected, the expression of *rcnA* was induced when aerobically grown bacteria were treated with 10 μ M Ni(II), but we observed no difference in the transcript levels in the Δ slyD strain compared to those in wild-type cells (Figure S13 of the Supporting Information). We next examined the transcript levels of *rcnA* in *E. coli* grown anaerobically with or without 10 μ M Ni(II) added to the growth media. Under these conditions, we also examined the expression levels of the *nik* operon, which encodes the NikABCDE Ni(II) importer that is upregulated during anaerobic growth,⁴³ when presumably it is pulling in Ni(II) required for the hydrogenase enzymes, and repressed by the transcription factor NikR in response to Ni(II).^{44,45} While a substantial induction in *rcnA* expression was observed upon metal supplementation of the growth medium, the changes in mRNA levels in the wild-type and Δ slyD strains were

comparable, indicating that SlyD does not modulate the nickel export pathway (Figure 6). In contrast, without Ni(II)

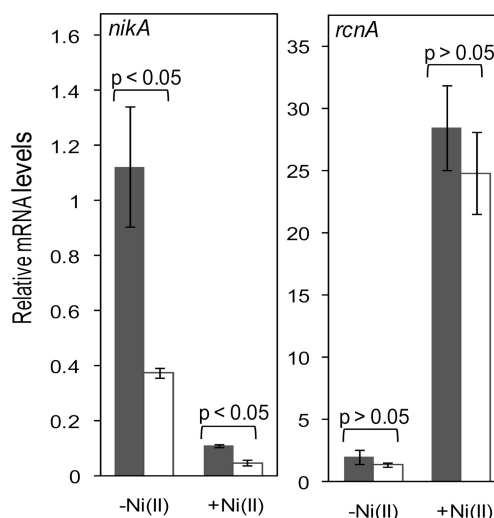


Figure 6. Expression of Ni(II) transporters in response to Ni(II). The mRNA levels from anaerobically cultured bacteria grown in minimal media optimized for hydrogenase expression without [−Ni(II)] or with 10 μ M Ni(II) [+Ni(II)] were measured. The amounts of mRNA observed in wild-type and Δ slyD strains are shown with gray and white bars, respectively. The observed transcript levels are relative to that of the DNA gyrase, *holB*. A *p* value (based on a Student's *t* test) of <0.05 indicates that the values are significantly different, and *p* values of >0.05 are considered not to be significantly different. Data are an average of three replicates.

supplementation of the media, an ~3-fold decrease in the *nikA* mRNA levels was detected in the Δ slyD strain when compared to that in the wild-type strain (Figure 6). Upon addition of 10 μ M Ni(II), an ~10-fold reduction in the level of expression of *nikA* was observed for the wild-type strain (Figure 6). Ni(II) also caused a decrease in the level of *nikA* transcription in the Δ slyD strain, such that the levels were approximately half of that of the wild-type cells grown under the same conditions. These diminished *nikA* transcript levels in the Δ slyD strain indicate an impact of SlyD on the Ni(II) uptake pathway.

To test whether SlyD contributes to nickel homeostasis specifically even in the presence of other metals, *nikA* and *rcnA* transcript levels were monitored in anaerobically grown bacteria treated for 30 min with 10 μ M Ni(II) as well as 400 μ M Zn(II), a concentration that is sufficiently high to elicit a response in zinc metalloregulators (see below). The amounts of mRNA of the two transporters followed a trend similar to that observed when the bacteria were treated with Ni(II) alone (Figure S14 of the Supporting Information), indicating that the impact of SlyD on the nickel pathways is not affected by the presence of excess zinc.

To determine whether SlyD can influence zinc homeostasis, the transcription of *znuA*, which encodes a subunit of the major inducible high-affinity Zn(II) uptake ABC transporter system, and *zntA*, which encodes a Zn(II) exporter from the P1-type ATPase family,² was monitored. The expression of these transporters is controlled by the metalloregulators Zur and ZntR, respectively.²² The concentration of Zn(II) used was chosen on the basis of the toxicity experiments, which revealed that 400 μ M Zn(II) results in slower growth (as opposed to a

lethal concentration leading to no growth). Furthermore, several previous investigations assessing the genome-wide transcriptional response of *E. coli* to zinc demonstrated that $>100 \mu\text{M}$ Zn(II) is sufficient to observe a change in the transcript levels of the above-mentioned transporters, albeit at different compositions of media.^{46,47} While the addition of Zn(II) led to an increase in the level of *zntA* transcription and a decrease in the level of *znuA* transcription, as expected, we observed no significant difference between wild-type and ΔslyD strains grown in the presence or absence of oxygen (Figures S13 and S15 of the Supporting Information).

We next tested the involvement of SlyD in copper homeostasis by examining *copA* and *cusF* transcripts upon addition of $150 \mu\text{M}$ Cu(II) to the medium in the presence of molecular oxygen. While the copper sensing transcription factor CueR regulates the expression of *copA*, *cusF* is under the control of the CusRS system.⁴⁸ Similar to that of Zn(II), this particular copper concentration was selected on the basis of our toxicity studies that indicated $150 \mu\text{M}$ is sufficient to reduce the growth rate of the bacteria. In addition, previous investigations of copper toxicity in *E. coli* by Outten et al. revealed that $>100 \mu\text{M}$ CuSO₄ is sufficient to cause extreme stress levels.⁴⁸ At these high copper concentrations, the primary copper exporter CopA and the CusCFBA system, which exports copper across both membranes, are necessary to render copper tolerance to the bacteria.⁴⁸ While the level of expression of both exporters increases in the presence of copper, *copA* transcripts are induced to a higher level compared to *cusF* in the presence of oxygen (Figure S13 of the Supporting Information). In contrast, in anaerobically grown bacteria, a more dramatic increase in mRNA levels was detected for *cusF* than for *copA* (Figure S15 of the Supporting Information), confirming the differential expression of the two exporters in response to molecular oxygen noted previously.⁴⁸ However, the mRNA levels were similar in the wild-type and ΔslyD strains, indicating that the lack of SlyD did not lead to perturbation of copper homeostasis in *E. coli* (Figures S13 and S15 of the Supporting Information).

DISCUSSION AND CONCLUSIONS

In this investigation, the in vitro metal-binding activities of *E. coli* SlyD and the impact of this protein on other metal homeostasis factors in vivo were examined. Among the metals tested, SlyD is capable of binding Zn(II), Cu(I), and Co(II) in vitro, as well as Ni(II), whereas Mn(II) and Fe(II) do not bind appreciably to isolated SlyD. On the basis of the in vitro studies, the order of preference of SlyD for metal ions is as follows: Mn(II) and Fe(II) < Co(II) < Ni(II) and Zn(II) \ll Cu(I). This series resembles the series of relative affinities observed for small molecule chelators for divalent metals, commonly termed the Irving–Williams series.⁴⁹ From these results, it is evident that the strength of metal binding is dictated by the properties of the metals rather than the protein and that SlyD is able to meet the coordination preferences of many of these metal ions. The fact that the sequence of SlyD does not impose selective metal binding on the protein is not surprising given the number and diversity of potential metal-binding residues in the MBD of SlyD (Figure S1 of the Supporting Information), allowing the protein to coordinate multiple ions of many of the first-row transition metals. In addition to the nondiscriminating primary structure, the lack of specificity is likely also due to the highly malleable conformation of the MBD, which is substantiated by the fact that the structure of this region cannot be resolved

from NMR measurements even upon addition of 1 equiv of Ni(II).⁶

Given the promiscuous and extensive metal binding capabilities of SlyD, it is reasonable to predict that it would contribute to the distribution of metals other than nickel in vivo. Deletion of *slyD* did not lead to a significant change in the transcription profiles of the copper or zinc transporters, suggesting that although the protein cannot preferentially coordinate Ni(II) over the other metals in vitro, its activity is specific for Ni(II) in vivo. Furthermore, the results from the RT-PCR and the toxicity studies clearly indicate that although the protein is capable of tightly coordinating multiple ions of several types of transition metals, SlyD does not function as a general metal detoxifier or buffer like some other Ni(II) storage factors such as Hpn or Hpn-like proteins.^{50,51} However, it is possible that SlyD may play a back-up role in metal sequestration and management when other metal transporters are severely compromised or overwhelmed, a hypothesis that remains to be tested.

When *E. coli* were grown in the presence of excess Zn(II) along with Ni(II), the influence of SlyD on the *nikA* mRNA levels was similar to that observed upon supplementation with Ni(II) alone. Thus, even toxic levels of Zn(II) that activate the cognate metalloregulators do not interfere with the impact of SlyD on nickel homeostasis. This result raises the question of how SlyD in vivo is able to overcome the preference for Zn(II) over Ni(II). One possible explanation involves metal-induced allostery.^{2,41} In this event, the binding of the “correct metal” is exploited to drive changes in the secondary, tertiary, and quaternary structure of the protein and/or dynamics (i.e., protein–protein interactions) that ultimately result in a biological function. For example, the coordination preferences of Ni(II) and Zn(II) are sufficiently different such that, even though the charge states observed in the ESI-MS data suggest similar overall changes in structure, it is likely that the two metals result in distinct protein folds, as indicated by the CD spectra. However, it is also clear that the effective intracellular concentrations of metal ions are tightly controlled within a cell. In *E. coli*, copper homeostasis is regulated by the copper sensor CueR, which has an estimated affinity for copper in the zeptomolar range (10^{-21} M).⁵² Similarly, the *E. coli* Zn(II) sensors Zur and ZntR bind their cognate metal with a K_D of $\sim 10^{-15}$ M.²² Such tight metal affinities of the regulators imply that all cellular copper and zinc is tightly bound and buffered within the cytosol. In support of this model, although Zn(II) can disrupt the Ni(II) binding capacity of SlyD in vitro, the lack of an impact of Zn(II) on the ability of SlyD to function in nickel homeostasis suggests a restricted availability of cytoplasmic zinc even when the bacteria are exposed to toxic zinc levels.

The differential impact of ΔslyD on the transcript levels of the Ni(II) importer *nikA* and the exporter *rcnA* provides several insights into the complex nickel homeostasis pathways in *E. coli*. Under anoxic conditions, the Nik transporter is expressed to establish a supply of nickel that meets the demands of the [NiFe]-hydrogenase enzymes.^{1,53} Deletion of *slyD* caused a downregulation of *nikA* transcription, with or without Ni(II) supplementation of the medium. This result is consistent with the previously reported observation that a ΔslyD strain of *E. coli* has a diminished level of uptake of ⁶³Ni(II) under anaerobic conditions.⁵ The smaller amounts of *nikA* imply a reduced Ni(II) capacity in the cytoplasm such that there is more nickel available to activate NikR. Deletion of SlyD would reduce the

number of Ni(II)-binding sites and thus weaken the ability of *E. coli* to sequester the Ni(II) imported by the Nik transporter. In addition, the Δ slyD strain has significantly less hydrogenase maturation,⁵ which would alleviate the demand for nickel ions. However, whether the decrease in the level of active hydrogenase is a consequence of the lower *nikA* levels, as opposed to a cause, is not clear. An analogous connection was observed upon treatment of *E. coli* with formate,⁵³ which activates hydrogenase production and decreases the level of repression of the *nik* promoter.

In contrast to the effect on NikR activity, deletion of *slyD* did not affect *rcnA* expression under any of the conditions investigated, indicating that SlyD does not influence the nickel-exporting pathway or the activity of the *rcnA* metal-lorepressor RcnR. In the absence of Ni(II) supplementation, the distinct effects of Δ slyD on the activities of NikR and RcnR could be explained by the higher affinity of NikR for Ni(II),^{33,44} such that it is more responsive than RcnR to changes in low levels of available metal. However, upon Ni(II) supplementation, a marked change in *rcnA* expression is observed, indicating that sufficient Ni(II) enters the cell to cause derepression by RcnR, but the *slyD* deletion still has no impact. These results support a model in which nickel is compartmentalized in the *E. coli* cytoplasm, resulting in two distinct pools of Ni(II) that are maintained by transcription factors RcnR and NikR.⁴² Furthermore, it appears that the role of SlyD is constrained to the nickel that is directed toward the hydrogenase biosynthetic pathway. The assignment of SlyD as a dedicated metallochaperone is in agreement with the observation that SlyD does not influence the sensitivity of *E. coli* to nickel toxicity, suggesting that the Ni(II) capacity of the protein is reserved for the maturation of the hydrogenase enzymes.

Although deletion of the genes for the Nik importer abrogates hydrogenase activity,⁴³ it does not affect the response of NikR to exogenous Ni(II), suggesting that metallochaperones sequester Ni(II) for hydrogenase maturation at the transporter.^{42,53} Given that disruption of *slyD* impacts the activity of NikR as well as hydrogenase maturation, it is likely that its role is not just as a source of nickel for the hydrogenase enzymes. SlyD forms a complex with the hydrogenase accessory protein HypB,⁵ so it is possible that it contributes to the biosynthetic pathway through this partnership. How it influences the communication between the hydrogenase-directed pool of Ni(II) and management of this pool by NikR will be a subject of future studies.

Similar to those of copper and zinc, nickel concentrations are thought to be tightly buffered within *E. coli*.⁴² Then how is SlyD able to bind Ni(II) in vivo and impact the homeostasis of this metal? NikR has two different Ni(II)-binding sites, with affinities of 10^{-12} and 10^{-7} M.¹ Binding of Ni(II) to both sites allows the regulator to bind to its recognition sequence in vitro with a tighter affinity than when only a single site is occupied by Ni(II),^{44,54} suggesting two levels of gene regulation. If one were to follow the above argument presented for Cu(I) and Zn(II) ion regulation, then SlyD, which chelates Ni(II) with an $\sim 10^{-10}$ M affinity, would not be able to compete with the high-affinity metal sites of NikR. However, it is possible that the protein is able to sequester enough metal for storage and/or transfer before the low-affinity site of NikR is filled and transcription of the nickel importer is completely turned off. On the other hand, if SlyD can interact in some fashion with the Nik transporter, there may be no such competition. Transfer of Ni(II) from the Nik transporter to SlyD, either directly or

indirectly, would circumvent the thermodynamically dictated metal affinities of competing proteins and ensure a population of protein loaded with nickel through kinetic control.

In conclusion, SlyD is a remarkable protein with a number of sites that will accept a variety of transition metals, but Ni(II) is the target metal in vivo. Utilizing metallochaperones for metal delivery and compartmentalization is a means of overcoming the thermodynamic preferences of proteins for metals. Further experiments are currently underway to determine the details of how SlyD contributes to the trafficking of nickel to the hydrogenase enzyme in *E. coli*.

■ ASSOCIATED CONTENT

§ Supporting Information

Experimental details of the competition titrations with PAR, Bcs, and Fura2; a summary of metal concentrations used for metal toxicity studies, a list of primers used for qRT-PCR analysis, and a summary of Mn(II), Co(II), and Ni(II) stoichiometries of SlyD (Tables S1–S3, respectively); representative spectra of Ni(II) titrations analyzed via ESI-MS (Figure S2); graphical representation of the PAR competition assay used for determining the average $K_{D[Ni(II)-SlyD]}$ and a comparison of CD spectra for Ni(II)- and Zn(II)-bound SlyD (Figures S3 and S4, respectively); representative data set for a Cu(I) titration of SlyD analyzed via electronic absorption spectroscopy (Figure S5); competition titrations with Bca and Bcs used for determining copper stoichiometry and affinity, respectively (Figures S6 and S7, respectively); graphical representations of Co(II) titrations analyzed via ESI-MS, competition titrations with Fura2 for determining average $K_{D[Co(II)-SlyD]}$ values, and titration of a cobalt-saturated SlyD sample with Zn(II) (Figures S8–S10, respectively); spectroscopy data obtained for titration of Ni(II) compared with a similar titration conducted in the presence of excess Fe(II) (Figure S11); representative growth curves of WT and Δ slyD strains determined in minimal medium supplemented with various amounts of metal (Figure S12); relative mRNA levels measured for various metal transporters under aerobic conditions (Figure S13); and relative mRNA levels measured for various metal transporters under anaerobic conditions (Figures S14 and S15). This material is available free of charge via the Internet at <http://pubs.acs.org>.

■ AUTHOR INFORMATION

Corresponding Author

*Phone and fax: (416) 978-3568. E-mail: dzamble@chem.utoronto.ca.

Present Address

[†]Max-Planck-Institut für Bioorganische Chemie, Stiftstrasse 34-36, 45470 Mülheim an der Ruhr, Germany.

Funding

This work was supported in part by funding from the Canadian Institutes of Health Research (D.B.Z.), the Natural Sciences and Engineering Research Council (NSERC) of Canada (M.J.S.), and the Canada Research Chairs program. We also thank NSERC for financial support through Graduate Scholarships for D.E.K.S. and H.K.

■ ACKNOWLEDGMENTS

We thank Prof. B. J. Andrews (University of Toronto) for her generous support in providing materials and instrumentation for gathering qRT-PCR data. We also thank Prof. A. Böck for

the donation of the MC4100 strains and Prof. A. Emili for the donation of the BW25113 strains.

ABBREVIATIONS

Bcs, bathocuproine sulfonate; Bca, bicinchoninate; ESI-MS, electrospray ionization mass spectrometry; EGTA, ethylene glycol tetraacetic acid; HSID, hot source-induced desolvation; MBD, metal-binding domain; PAR, 4-(2-pyridylazo)resorcinol; WT, wild-type.

REFERENCES

- (1) Li, Y., and Zamble, D. B. (2009) Nickel homeostasis and nickel regulation: An overview. *Chem. Rev.* 109, 4617–4643.
- (2) Waldron, K. J., and Robinson, N. J. (2009) How do bacterial cells ensure that metalloproteins get the correct metal? *Nat. Rev. Microbiol.* 7, 25–35.
- (3) Robinson, N. J. (2007) A more discerning zinc exporter. *Nat. Chem. Biol.* 3, 692–693.
- (4) Leach, M. R., and Zamble, D. B. (2007) Metallocenter assembly of the hydrogenase enzymes. *Curr. Opin. Chem. Biol.* 11, 159–165.
- (5) Zhang, J. W., Butland, G., Greenblatt, J. F., Emili, A., and Zamble, D. B. (2005) A role for SlyD in the *Escherichia coli* hydrogenase biosynthetic pathway. *J. Biol. Chem.* 280, 4360–4366.
- (6) Martino, L., He, Y., Hands-Taylor, K. L., Valentine, E. R., Kelly, G., Giancola, C., and Conte, M. R. (2009) The interaction of the *Escherichia coli* protein SlyD with nickel ions illuminates the mechanism of regulation of its peptidyl-prolyl isomerase activity. *FEBS J.* 276, 4529–4544.
- (7) Weininger, U., Haupt, C., Schweimer, K., Graubner, W., Kovermann, M., Bruser, T., Scholz, C., Schaarschmidt, P., Zoldak, G., Schmid, F. X., and Balbach, J. (2009) NMR solution structure of SlyD from *Escherichia coli*: Spatial separation of prolyl isomerase and chaperone function. *J. Mol. Biol.* 387, 295–305.
- (8) Knappe, T. A., Eckert, B., Schaarschmidt, P., Scholz, C., and Schmid, F. X. (2007) Insertion of a chaperone domain converts FKBP12 into a powerful catalyst of protein folding. *J. Mol. Biol.* 368, 1458–1468.
- (9) Scholz, C., Eckert, B., Hagn, F., Schaarschmidt, P., Balbach, J., and Schmid, F. X. (2006) SlyD proteins from different species exhibit high prolyl isomerase and chaperone activities. *Biochemistry* 45, 20–33.
- (10) Jakob, R. P., Zoldak, G., Aumuller, T., and Schmid, F. X. (2009) Chaperone domains convert prolyl isomerases into generic catalysts of protein folding. *Proc. Natl. Acad. Sci. U.S.A.* 106, 20282–20287.
- (11) Zoldak, G., and Schmid, F. X. (2011) Cooperation of the prolyl isomerase and chaperone activities of the protein folding catalyst SlyD. *J. Mol. Biol.* 406, 176–194.
- (12) Erdmann, F., and Fischer, G. (2007) The nickel-regulated peptidyl prolyl cis/trans isomerase SlyD. In *Metal Ions in Life Sciences* (Sigel, A., Sigel, H., and Sigel, R. K. O., Eds.) pp 501–518, John Wiley and Sons, New York.
- (13) Leach, M. R., Zhang, J. W., and Zamble, D. B. (2007) The role of complex formation between the *Escherichia coli* hydrogenase accessory factors HypB and SlyD. *J. Biol. Chem.* 282, 16177–16186.
- (14) Kaluarachchi, H., Sutherland, D. E., Young, A., Pickering, I. J., Stillman, M. J., and Zamble, D. B. (2009) The Ni(II)-Binding Properties of the Metallochaperone SlyD. *J. Am. Chem. Soc.* 131, 18489–18500.
- (15) Wulfig, C., Lombardero, J., and Pluckthun, A. (1994) An *Escherichia coli* protein consisting of a domain homologous to FK506-binding proteins (FKBP) and a new metal binding motif. *J. Biol. Chem.* 269, 2895–2901.
- (16) Finney, L. A., and O'Halloran, T. V. (2003) Transition metal speciation in the cell: Insights from the chemistry of metal ion receptors. *Science* 300, 931–936.
- (17) Salgado, M. T., Bacher, K. L., and Stillman, M. J. (2007) Probing the structural change in the α and β domains of copper- and silver-substituted metallothionein by emission spectroscopy and electrospray ionization mass spectrometry. *J. Biol. Inorg. Chem.* 12, 294–312.

- (18) Zimmermann, M., Clarke, O., Gulbis, J. M., Keizer, D. W., Jarvis, R. S., Cobbett, C. S., Hinds, M. G., Xiao, Z. G., and Wedd, A. G. (2009) Metal Binding Affinities of *Arabidopsis* Zinc and Copper Transporters: Selectivities Match the Relative, but Not the Absolute, Affinities of their Amino-Terminal Domains. *Biochemistry* 48, 11640–11654.
- (19) Atanassova, A., Lam, R., and Zamble, D. B. (2004) A high-performance liquid chromatography method for determining transition metal content in proteins. *Anal. Biochem.* 335, 103–111.
- (20) Baba, T., Ara, T., Hasegawa, M., Takai, Y., Okumura, Y., Baba, M., Datsenko, K. A., Tomita, M., Wanner, B. L., and Mori, H. (2006) Construction of *Escherichia coli* K-12 in-frame, single-gene knockout mutants: The Keio collection. *Mol. Syst. Biol.* 2, 2006.0008.
- (21) Graham, A. I., Hunt, S., Stokes, S. L., Bramall, N., Bunch, J., Cox, A. G., McLeod, C. W., and Poole, R. K. (2009) Severe Zinc Depletion of *Escherichia coli*: Roles for High Affinity Zinc Binding by ZinT, Zinc Transport and Zinc-Independent Proteins. *J. Biol. Chem.* 284, 18377–18389.
- (22) Outten, C. E., and O'Halloran, T. V. (2001) Femtomolar sensitivity of metalloregulatory proteins controlling zinc homeostasis. *Science* 292, 2488–2492.
- (23) Ngu, T. T., and Stillman, M. J. (2009) Metal-binding mechanisms in metallothioneins. *Dalton Trans.*, 5425–5433.
- (24) Kaltashov, I. A., and Abzalimov, R. R. (2008) Do ionic charges in ESI MS provide useful information on macromolecular structure? *J. Am. Soc. Mass Spectrom.* 19, 1239–1246.
- (25) Tanaka, M., Funahashi, S., and Shirai, K. (1968) Kinetics of Ligand Substitution Reaction of Zinc(2)-4-(2-Pyridylazo)Resorcinol Complex with (Ethylene Glycol)Bis(2-Aminoethyl Ether)-N,N,N',N'-Tetraacetic Acid. *Inorg. Chem.* 7, 573–578.
- (26) McNulty, T. J., and Taylor, C. W. (1999) Extracellular heavy-metal ions stimulate Ca^{2+} mobilization in hepatocytes. *Biochem. J.* 339, 555–561.
- (27) Hottenrott, S., Schumann, T., Pluckthun, A., Fischer, G., and Rahfeld, J. U. (1997) The *Escherichia coli* SlyD is a metal ion-regulated peptidyl-prolyl cis/trans-isomerase. *J. Biol. Chem.* 272, 15697–15701.
- (28) Perczel, A., Hollosi, M., and Fasman, G. D. (1996) *Circular Dichroism and the Conformational Analysis of Biomolecules*, Springer, New York.
- (29) Rensing, C., and Grass, G. (2003) *Escherichia coli* mechanisms of copper homeostasis in a changing environment. *FEMS Microbiol. Rev.* 27, 197–213.
- (30) Cobine, P. A., George, G. N., Jones, C. E., Wickramasinghe, W. A., Solioz, M., and Dameron, C. T. (2002) Copper transfer from the Cu(I) chaperone, CopZ, to the repressor, Zn(II)CopY: Metal coordination environments and protein interactions. *Biochemistry* 41, 5822–5829.
- (31) Badarau, A., Firbank, S. J., McCarthy, A. A., Banfield, M. J., and Dennison, C. (2010) Visualizing the Metal-Binding Versatility of Copper Trafficking Sites. *Biochemistry* 49, 7798–7810.
- (32) Xiao, Z., Brose, J., Schimo, S., Ackland, S. M., La Fontaine, S., and Wedd, A. G. (2011) Unification of the Copper(I) Binding Affinities of the Metallo-chaperones Atx1, Atox1, and Related Proteins: Detection Probes and Affinity Standards. *J. Biol. Chem.* 286, 11047–11055.
- (33) Iwig, J. S., Leitch, S., Herbst, R. W., Maroney, M. J., and Chivers, P. T. (2008) Ni(II) and Co(II) sensing by *Escherichia coli* RcnR. *J. Am. Chem. Soc.* 130, 7592–7606.
- (34) Koch, D., Nies, D. H., and Grass, G. (2007) The RcnRA (YohLM) system of *Escherichia coli*: A connection between nickel, cobalt and iron homeostasis. *BioMetals* 20, 759–771.
- (35) Rodrigue, A., Effantin, G., and Mandrand-Berthelot, M. A. (2005) Identification of *rcnA* (*yohM*), a nickel and cobalt resistance gene in *Escherichia coli*. *J. Bacteriol.* 187, 2912–2916.
- (36) Wang, S. C., Dias, A. V., Bloom, S. L., and Zamble, D. B. (2004) Selectivity of metal binding and metal-induced stability of *Escherichia coli* NikR. *Biochemistry* 43, 10018–10028.
- (37) Golynskiy, M. V., Gunderson, W. A., Hendrich, M. P., and Cohen, S. M. (2006) Metal binding studies and EPR spectroscopy of

the manganese transport regulator MntR. *Biochemistry* 45, 15359–15372.

(38) Kwan, C. Y., and Putney, J. W. (1990) Uptake and Intracellular Sequestration of Divalent-Cations in Resting and Methacholine-Stimulated Mouse Lacrimal Acinar-Cells: Dissociation by Sr^{2+} and Ba^{2+} of Agonist-Stimulated Divalent-Cation Entry from the Refilling of the Agonist-Sensitive Intracellular Pool. *J. Biol. Chem.* 265, 678–684.

(39) Grynkiewicz, G., Poenie, M., and Tsien, R. Y. (1985) A new generation of Ca^{2+} indicators with greatly improved fluorescence properties. *J. Biol. Chem.* 260, 3440–3450.

(40) Morleo, A., Bonomi, F., Iametti, S., Huang, V. W., and Kurtz, D. M. Jr. (2010) Iron-nucleated folding of a metalloprotein in high urea: Resolution of metal binding and protein folding events. *Biochemistry* 49, 6627–6634.

(41) Giedroc, D. P., and Arunkumar, A. I. (2007) Metal sensor proteins: Nature's metalloregulated allosteric switches. *Dalton Trans.* 29, 3107–3120.

(42) Iwig, J. S., Rowe, J. L., and Chivers, P. T. (2006) Nickel homeostasis in *Escherichia coli*: The *rcnR-rcnA* efflux pathway and its linkage to NikR function. *Mol. Microbiol.* 62, 252–262.

(43) Wu, L. F., Mandrand-Berthelot, M. A., Waugh, R., Edmonds, C. J., Holt, S. E., and Boxer, D. H. (1989) Nickel deficiency gives rise to the defective hydrogenase phenotype of *hydC* and *fir* mutants in *Escherichia coli*. *Mol. Microbiol.* 3, 1709–1718.

(44) Chivers, P. T., and Sauer, R. T. (2000) Regulation of high affinity nickel uptake in bacteria. Ni^{2+} -Dependent interaction of NikR with wild-type and mutant operator sites. *J. Biol. Chem.* 275, 19735–19741.

(45) De Pina, K., Desjardin, V., Mandrand-Berthelot, M. A., Giordano, G., and Wu, L. F. (1999) Isolation and characterization of the *nikR* gene encoding a nickel-responsive regulator in *Escherichia coli*. *J. Bacteriol.* 181, 670–674.

(46) Lee, L. J., Barrett, J. A., and Poole, R. K. (2005) Genome-wide transcriptional response of chemostat-cultured *Escherichia coli* to zinc. *J. Bacteriol.* 187, 1124–1134.

(47) Yamamoto, K., and Ishihama, A. (2005) Transcriptional response of *Escherichia coli* to external zinc. *J. Bacteriol.* 187, 6333–6340.

(48) Outten, F. W., Huffman, D. L., Hale, J. A., and O'Halloran, T. V. (2001) The independent cue and cus systems confer copper tolerance during aerobic and anaerobic growth in *Escherichia coli*. *J. Biol. Chem.* 276, 30670–30677.

(49) Irving, H., and Williams, R. J. P. (1948) Order of Stability of Metal Complexes. *Nature* 162, 746–747.

(50) Ge, R., Zhang, Y., Sun, X., Watt, R. M., He, Q. Y., Huang, J. D., Wilcox, D. E., and Sun, H. (2006) Thermodynamic and kinetic aspects of metal binding to the histidine-rich protein, Hpn. *J. Am. Chem. Soc.* 128, 11330–11331.

(51) Zeng, Y. B., Yang, N., and Sun, H. (2011) Metal-binding properties of an hpn-like histidine-rich protein. *Chemistry* 17, 5852–5860.

(52) Changela, A., Chen, K., Xue, Y., Holschen, J., Outten, C. E., O'Halloran, T. V., and Mondragon, A. (2003) Molecular basis of metal-ion selectivity and zeptomolar sensitivity by CueR. *Science* 301, 1383–1387.

(53) Rowe, J. L., Starnes, G. L., and Chivers, P. T. (2005) Complex transcriptional control links NikABCDE-dependent nickel transport with hydrogenase expression in *Escherichia coli*. *J. Bacteriol.* 187, 6317–6323.

(54) Bloom, S. L., and Zamble, D. B. (2004) Metal-selective DNA-binding response of *Escherichia coli* NikR. *Biochemistry* 43, 10029–10038.